Membrane Morphogenesis in Retinal Rod Outer Segments: Inhibition by Tunicamycin

STEVEN J. FLIESLER, MARY E. RAYBORN, and JOE G. HOLLYFIELD
Cullen Eye Institute, Baylor College of Medicine, Houston, Texas 77030. Dr. Fliesler's present address is Bascom Palmer Eye Institute, Miami, Florida 33101.

ABSTRACT Isolated *Xenopus laevis* retinas were incubated with ^{3}H-labeled mannose or leucine in the presence or absence of tunicamycin (TM), a selective inhibitor of dolichyl phosphate-dependent protein glycosylation. At a TM concentration of 20 μg/ml, the incorporation of [^{3}H]mannose and [^{3}H]leucine into retinal macromolecules was inhibited by ~66 and 12–16%, respectively, relative to controls. Cellular uptake of the radiolabeled substrates was not inhibited at this TM concentration. Polyacrylamide gel electrophoresis revealed that TM had little effect on the incorporation of [^{3}H]leucine into the proteins of whole retinas and that labeling of proteins (especially opsin) in isolated rod outer segment (ROS) membranes was negligible. The incorporation of [^{3}H]mannose into proteins of whole retinas and ROS membranes was nearly abolished in the presence of TM. Autoradiograms of control retinas incubated with either [^{3}H]mannose or [^{3}H]leucine exhibited a discrete concentration of silver grains over ROS basal disc membranes. In TM-treated retinas, the extracellular space between rod inner and outer segments was dilated and filled with numerous heterogeneously size vesicles, which were labeled with [^{3}H]leucine but not with [^{3}H]mannose. ROS disc membranes per se were not labeled in the TM-treated retinas. Quantitative light microscopic autoradiography of retinas pulse-labeled with [^{3}H]leucine showed no differences in labeling of rod cellular compartments in the presence or absence of TM as a function of increasing chase time. These results demonstrate that TM can block retinal protein glycosylation and normal disc membrane assembly under conditions where synthesis and intracellular transport of rod cell proteins (e.g., opsin) are not inhibited.

The rod photoreceptor in the vertebrate retina is a structurally and functionally polarized and segmented postmitotic cell. The rod outer segment (ROS)[1] is composed of a highly ordered stack of individual, flattened double-membrane saccules (the disc membranes) enveloped by the plasma membrane of the cell. The photosensitive nature of the ROS is due to the presence of rhodopsin, the rod visual pigment, in the disc membranes. The ROS is attached to the adjacent rod inner segment (RIS) by the connecting cilium, a narrow cytoplasmic bridge through which intracellular exchange and flow of cytoplasmic constituents takes place. The RIS, which contains the organelles of anabolic and catabolic metabolism, is compartmentalized into two regions: the ellipsoid and the myoid. The ellipsoid (proximal to the connecting cilium) is filled with a dense cluster of mitochondria, whereas the myoid (distal to the nucleus) houses an extensive network of endoplasmic reticulum and the Golgi apparatus.

The rod cell renews the ROS membranes at a prodigious rate in an ongoing process throughout its lifetime (47, 64, 65). For instance, in the African clawed toad *Xenopus laevis*, ~80 disc membranes (each containing ~1 × 10^6 rhodopsin molecules) are added to the ROS daily (6, 25). Since the ROS is devoid of the cellular machinery required for *de novo* synthesis of macromolecules, it must rely upon the RIS for its supply of new membrane precursors. Classically, the biogenesis of ROS membranes has been studied by examination of the sequential synthesis, processing, and intracellular transport of opsin (the visual pigment apoprotein), which precede its assembly into newly forming ROS disc membranes (for a review, see references 40, 47, and 60, and literature cited therein). Opsin is initially synthesized in the endoplasmic reticulum of the rod cell and is then sequentially transported

[1] *Abbreviations used in this paper*: ITV, intracellular transport vesicle; TCA, trichloroacetic acid; RIS, rod inner segment; ROS, rod outer segment.

THE JOURNAL OF CELL BIOLOGY · VOLUME 100 FEBRUARY 1985 574-587

through the myoid (via the Golgi apparatus) and the ellipsoid regions of the RIS to the site of assembly of disc membranes at the base of the ROS (4, 8, 9, 18, 19, 41, 42, 64). Biochemical and autoradiographic studies have shown that glycosylation of newly synthesized opsin takes place initially in the rough endoplasmic reticulum, with the subsequent addition of glucosamine (i.e., the terminal GlcNAc residue) in the Golgi apparatus (8, 9, 38). Subcellular fractionation and biochemical analysis of retinas after pulse-chase incubations has revealed that opsin is always membrane bound during its migration through the RIS to the ROS (45). Immunocytochemical electron microscopic studies have demonstrated the presence of opsin in the endoplasmic reticulum, Golgi apparatus, and intracellular transport vesicles (ITVs) in the ellipsoid and periciliary RIS cytoplasm, as well as in the ROS membranes (48, 49). The prevalent model for disc morphogenesis involves the fusion of opsin-containing ITVs with the RIS plasma membrane, then lateral diffusion of opsin vectorially to the base of the ROS (see references 47, 50, and 57, and literature cited therein). Although the mechanical details remain obscure, the expansion of the basal ROS plasma membrane caused by the addition of new material results in deformation and evagination of the plasma membrane to form contiguous open discs. The apposing membrane lamellae of the open discs fuse at their outer margins and subsequently detach from the plasma membrane, thereby adding to the stack of closed discs enveloped by the ROS plasma membrane.

Opsin is composed of a moderate-sized ($M_r \sim 39{,}000$) single polypeptide chain to which two unusually short asparagine-linked oligosaccharide chains are covalently coupled (16, 20, 33). The oligosaccharide chains of opsin, which are composed of mannose and *N*-acetylglucosamine (16, 33, 51), are structurally similar to the core oligosaccharide moiety common to the *N*-glycosidically linked oligosaccharides of other, more extensively glycosylated proteins (30, 36). The synthesis of *N*-glycosidically linked oligosaccharides is a highly complex process which involves elaboration of a precursor oligosaccharide on a long chain polyprenyl lipid, dolichyl phosphate (54, 56, 58, 59). The precursor oligosaccharide is transfered from dolichyl phosphate to an asparagine residue within the *N*-terminal region of a nascent polypeptide acceptor in the rough endoplasmic reticulum. Post-translational modifications of the oligosaccharide (i.e., trimming of terminal sugars and addition of other sugars to form more complex structures) do not involve dolichyl phosphate and take place in other cellular compartments (i.e., more distal domains of the endoplasmic reticulum, the Golgi apparatus, and the plasma membrane) (54, 56, 59). Various enzymatic and biochemical aspects of this lipid intermediate pathway have been demonstrated in retinal tissue (reference 28 and literature cited therein). Recently, it has been shown that the biogenic activity of the lipid intermediate pathway in the retina is highest in the photoreceptor cells (15).

In both bovine (52) and *Rana pipiens* retinas (12) in vitro it has been demonstrated that tunicamycin (TM), a relatively selective inhibitor of the lipid intermediate pathway (11, 32, 56, 58–61, 63), can block the glycosylation of opsin, resulting in the formation of a nonglycosylated polypeptide of a slightly lower apparent M_r. In the study employing bovine retinas (52), the association of radiolabeled nonglycosylated opsin with ROS membranes isolated from retinas that had been incubated with radiolabeled glycoprotein precursors in the presence of TM suggested that glycosylation of opsin was not required for its incorporation into ROS membranes. However, these results are also consistent with alternative explanations, e.g., comigration or fusion of radiolabeled RIS-derived membranes containing newly synthesized, nonglycosylated opsin with unlabeled, previously formed ROS membranes during the isolation procedures. In this regard, electron microscopic and immunocytochemical studies have revealed the presence of opsin-containing vesicles in the periciliary region of the RIS cytoplasm, proximal to the ROS (7, 29, 47, 48). In contrast, biochemical and light microscopic autoradiographic evidence from the study using *Rana* retinas (12) demonstrated that TM-mediated inhibition of opsin glycosylation resulted in a lack of assembly of opsin into new ROS membranes. The mechanical details involved in this inhibition of ROS membrane assembly, however, were not defined. We examined the effects of TM on the in vitro incorporation of radiolabeled precursors into glycoproteins destined for ROS membrane assembly in *Xenopus* retinas, using light and electron microscopic autoradiography and biochemical methods. Our results confirm those of a previous study (12) that suggested that glycosylation is required for the normal assembly of opsin into ROS disc membranes. Furthermore, we show that in TM-treated retinas, membrane proteins originally destined for the ROS but lacking their normal complement of *N*-linked oligosaccharides are exported from the rod cell into the extracellular space in the form of membrane vesicles. Preliminary accounts of these studies have been presented elsewhere (13, 14).

MATERIALS AND METHODS

Animals and Reagents: Young adult *X. laevis* (Nasco Biologicals, Ft. Atkinson, WI) were maintained at 21°C in constant temperature incubators under cyclic lighting (12 h dark, 12 h light) for at least 2 wk before use. TM (Calbiochem-Behring Corp., La Jolla, CA) was dissolved in dimethylsulfoxide (Burdick & Jackson Laboratories Inc., Hoffmann-La Roche, Inc., Muskegon, MI) to obtain a stock solution (10 mg/ml). Amphibian tissue culture medium (Wolf-Quimby Medium) was purchased from Gibco Laboratories (Grand Island, NY). The radiolabeled substrates L-[4,5-^{3}H]leucine (52–136 Ci/mmol) and D-[2,6-^{3}H]mannose (32–44 Ci/mmol) were obtained from Amersham Corp. (Arlington Heights, IL). A mixture of U-^{14}C-labeled amino acids (protein hydrolysate; specific activity range 151–460 mCi/mmol) was obtained from Schwarz/Mann (Spring Valley, NY). Reagents for polyacrylamide gel electrophoresis and standard proteins of known molecular weight were purchased from Bio-Rad Laboratories (Richmond, CA).

Incubation of Retinas: Animals were adapted to dark ovenight and retinas were dissected free of pigment epithelium under dim red light within 1 h before the time of normal light onset. Groups of retinas (16–30 per flask, in 10 ml of medium) were pre-incubated (i.e., in the absence of radiolabeled substrates) at 21°C under 95% O_2/5% CO_2 atmosphere in darkness for 1 h as previously described (27) in the presence or absence of TM. This pre-incubation allowed the TM to equilibrate with the tissue. The culture medium was a modified Ringer's bicarbonate solution (4), with 20 mM sodium pyruvate substituted for 10 mM glucose, and supplemented with 25% (vol/vol) amphibian tissue culture medium. Aliquots of the stock solution of TM were added in order to obtain a final TM concentration of 20 μg/ml and a dimethylsulfoxide concentration of 0.2% (vol/vol) in the culture medium (control medium contained 0.2% dimethylsulfoxide alone). Retinas were then transferred to flasks and pulse-labeled for 1 h in darkness in medium containing either [^{3}H]-leucine (0.1 mCi/ml) or [^{3}H]mannose (0.5 mCi/ml), with or without TM. After gentle and rapid rinsing of the retinas through four changes of ice-chilled culture medium (10 ml each), a chase incubation was carried out in flasks containing 10 ml of fresh medium (supplemented with 0.1 mM L-leucine and 5 mM D-mannose, with or without TM) for an additional 4 h under normal fluorescent room lighting. Incubations were terminated by immersion of the flasks in an ice-water bath immediately before the tissue was processed for analysis.

Microscopy and Autoradiography: Retinas were fixed overnight in chilled 0.1 M cacodylate buffer (pH 7.4) containing 0.025% $CaCl_2$, 2%

glutaraldehyde, and 2% formaldehyde. The procedures for further processing of retinas for light and electron microscopy, autoradiography, and quantitation of autoradiograms have been described in detail elsewhere (26, 27). At least three retinas were analyzed for each treatment or recovery time; at least three sections per retina and at least 20 photoreceptors per section were used for quantitative autoradiography.

Biochemical Methods: Retinas (at least three per treatment or time point) were cut in half with a razor blade. Total retinal proteins of individual halves were precipitated in ice-chilled 10% trichloroacetic acid (TCA), and the TCA-precipitable material was solubilized in 1 N NaOH. The specific radioactivity (disintegrations per minute per microgram protein) was determined by liquid scintillation counting and by fluorometric assay of protein content with fluorescamine (62), as described previously (35). The remaining half-retinas were pooled, solubilized in Laemmli sample buffer (31), and analyzed by polyacrylamide gel electrophoresis in the presence of sodium dodecyl sulfate (SDS PAGE), by use of a discontinuous 7.5:15% gradient slab gel system as described in detail elsewhere (15, 35). Coomassie Blue staining and fluorography of gels was performed as previously described (15, 35).

Measurement of Substrate Uptake: To examine the effects of TM on the uptake of radiolabeled glycoprotein precursors by retinal cells, dark-adapted retinas (5 per flask) were pre-incubated as described above for 1 h and then pulse-labeled for 10 min with [^{3}H]mannose (60 μCi/ml) and a mixture of ^{14}C-labeled amino acids (7 μCi/ml) in the presence or absence of TM (20 μg/ml, 0.2% dimethylsulfoxide. After rapid rinsing through four changes of ice-chilled chase medium, retinas were individually precipitated with TCA, and the incorporation of ^{3}H and ^{14}C into total retinal TCA-soluble material (normalized to the TCA-precipitable protein content) was determined (15, 35).

Preparation of ROS Membranes: In some experiments, retinas were incubated with [^{3}H]leucine or [^{3}H]mannose by use of the pulse-chase protocol described above, and ROS membranes were isolated and purified by discontinuous sucrose gradient centrifugation by a modification of the method of Papermaster and Dreyer (48). Retinas were placed into 17-ml capacity cellulose nitrate tubes containing 3.0 ml of ice-chilled 42% (wt/wt) sucrose (d = 1.19 g/cm^3) and gently vortexed at low speed for 30 s. The resulting suspension of partially fragmented retinas was overlayered with buffered sucrose solutions (containing 10 mM Tris-acetate, pH 7.4, and 5 mM $MgCl_2$) of the following densities (grams per cubic centimeter): 1.15 (3.0 ml), 1.13 (6.0 ml), and 1.11 (4.0 ml). After centrifugation in a swinging-bucket rotor (1 h at 100,000 g, 4°C), the material that accumulated at the 1.11/1.13 g/cm^3 interface (ROS membranes) was harvested with a Pasteur pipet, diluted with 10 mM Tris-acetate buffer, pH 7.4, and centrifuged (30 min at 40,000 g, 4°C) in a fixed-angle rotor. The ROS membrane pellet was washed three times with buffer and collected by centrifugation as described above. The membranes were solubilized and analyzed by SDS PAGE.

Time Course of TM Effects: To ascertain whether or not TM affected the viability of retinas over the time course of these studies, retinas (3 per time point) were pre-incubated for 1 h as described above and then incubated with [^{3}H]leucine (0.1 mCi/ml) in the presence or absence of TM for various periods (i.e., 0.5, 1, 2, 4 and 6 h). After rinsing was done, the specific activity of the total retinal TCA-precipitable material was determined as described above.

A time course for the effects of TM on the morphology of the rod photoreceptor cells was also obtained by fixation of retinas at various intervals of incubation (i.e., 1, 2, 4, and 6 h) and analysis of the tissue by electron microscopy.

RESULTS

Retina Viability and Differential Inhibition of Protein Glycosylation vs. Polypeptide Synthesis in the Presence of TM

The specific inhibitory effect of TM is exerted upon the enzyme that catalyzes the first reaction in the lipid intermediate pathway, namely UDP-*N*-acetylglucosamine/dolichylphosphate *N*-acetylglucosamine-1-phosphate transferase (32, 58, 60, 61). Prevention of the formation of the first lipid-saccharide intermediate in the synthesis of oligosaccharides destined to be covalently joined via *N*-glycosidic linkages to nascent polypeptide acceptors blocks the overall synthesis of those oligosaccharides (and, therefore, the *N*-glycosylation of polypeptides). However, above a given concentration of TM, the relative magnitude of nonspecific inhibitory effects of TM (e.g., inhibition of polypeptide synthesis) increases (56, 59, 63). In addition, commercial preparations of TM are known to contain a heterogeneous mixture of structurally related compounds whose relative biologic activities vary with respect to the specific inhibition of the lipid intermediate pathway as well as the nonspecific inhibition of other metabolic pathways (10). As the relative magnitude of the nonspecific inhibitory effects increases, TM becomes generally cytotoxic. Therefore, it is essential to establish a concentration of TM that, for the given tissue and culture conditions, causes a maximal inhibition of protein glycosylation without producing significant nonspecific inhibitory effects.

TABLE I

*Effects of TM on Incorporation of ^{3}H-labeled Precursors into Retinal TCA-precipitable Material**

Substrate	TM	Specific activity		Percent of control**	
		Exp. 1	Exp. 2	Exp. 1	Exp. 2
		dpm/μg protein			
[^{3}H]Mannose	−	248	249	100.0	100.0
	+	83	85	33.5	34.0
[^{3}H]Leucine	−	460	1,284	100.0	100.0
	+	387	1,128	84.1	87.9

* Retinas were pre-incubated for 1 h, then pulse-labeled with either [^{3}H]-mannose (0.5 mCi/ml) or [^{3}H]leucine (0.1 mCi/ml) for 1 h, and chased for 4 h. TM concentration, 20 μg/ml.

** Values represent the average of triplicate determinations from two independent samples per experiment.

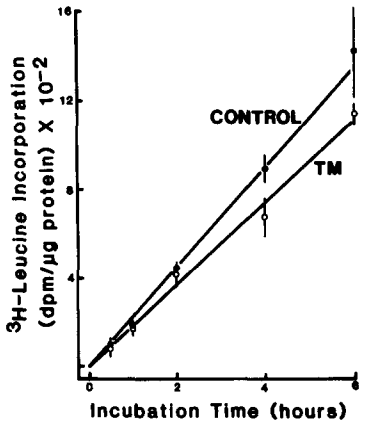

FIGURE 1 Incubation time course for [^{3}H]leucine incorporation into retina TCA-precipitable material in the presence (○) and absence (●) of TM.

Table I shows the data from two individual experiments in which retinas were incubated with either [^{3}H]leucine or [^{3}H]-mannose in the presence or absence of TM. Whereas the incorporation of [^{3}H]mannose into total retinal TCA-precipitable material was inhibited by 66% (relative to controls) in both cases, [^{3}H]leucine incorporation (a general indicator of polypeptide synthesis) was inhibited by only 12–16%. The differences in the actual specific activities obtained for [^{3}H]-leucine incorporation when the two experiments are compared are due to the fact that the specific activity of the [^{3}H]-leucine used in the second incubation was approximately threefold higher than in the first incubation. Thus, under the given experimental conditions, TM at a concentration of 20 μg/ml markedly inhibited protein glycosylation without significantly inhibiting polypeptide synthesis per se.

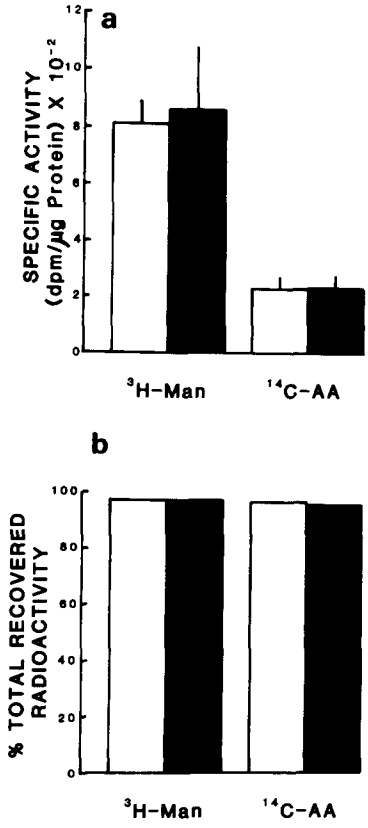

FIGURE 2 Effect of TM on the uptake of [^{3}H]mannose (*^{3}H-Man*) and ^{14}C-labeled amino acids (*^{14}C-AA*) by retinas. Open bars, controls; shaded bars, tunicamycin. (*a*) TCA-soluble radioactivity normalized to protein content of TCA-precipitable material (mean ± SD, n = 5). (*b*) TCA-soluble radioactivity expressed as a percentage of total recovered radioactivity (TCA-soluble plus TCA-precipitable radioactivity; mean ± SD, n = 5).

As a measure of the viability of the retinas under the employed experimental conditions, we monitored the incorporation of [^{3}H]leucine into retinal proteins (i.e., total TCA-precipitable material) as a function of incubation time in the presence and absence of TM. The results are shown in Fig. 1. The incorporation of [^{3}H]leucine increased linearly as a function of time in the presence and absence of TM. Thus, retinas incubated in the presence of TM under the given conditions remained viable throughout the incubation (6 h total). When the slopes of the two lines were compared, it was apparent that the rate of incorporation of [^{3}H]leucine in the retinas incubated with TM was ~20% less than that of the controls. An analysis of covariance, however, indicated that the divergence in the two rates became statistically significant ($P < 0.01$, $n = 3$) only after 2 h. This implies that under the given pulse-chase conditions (i.e., 1 h of pre-incubation with TM followed by a 1 h pulse with radiolabeled substrate and variable chase times), retinal proteins should achieve comparable specific activities in the presence or absence of TM during the pulse phase. This condition is necessary for any meaningful quantitative comparisons of autoradiograms in such pulse-chase protocols, as will be described later.

Effect of TM on Cellular Uptake of Radiolabeled Substrates

It is conceivable that the observed effects of TM on the incorporation of the radiolabeled glycoprotein precursors (especially [^{3}H]mannose) might be due to inhibition of the cellular uptake mechanisms for these substrates, which would result in a decrease in the specific activities of the intracellular substrate pools used for glycoprotein synthesis. Therefore, we examined the effect of TM on substrate uptake, using a dual-label protocol with [^{3}H]mannose and a mixture of ^{14}C-labeled amino acids. By choosing a relatively short pulse-labeling period (10 min), we established the conditions of uptake such that the form of the cellular radioactivity would be almost exclusively TCA soluble, in order to separate this process from subsequent incorporation of the intracellular substrates into TCA-precipitable macromolecules. Since the content of protein in the TCA-soluble material was below the level of detection for the protein assay employed, we normalized the absolute amount of TCA-soluble radioactivity to the TCA-precipitable protein content to obtain specific radioactivity values. The results are shown in Fig. 2. Under the conditions employed, ~97% of the total recovered radioactivity (TCA-soluble plus TCA-precipitable material) was present in the TCA-soluble fraction in the presence and absence of TM (Fig. 2*b*). There was no statistically significant difference in the specific activity of the TCA-soluble material in the presence or absence of TM (Fig. 2*a*). Therefore, TM did not significantly perturb cellular uptake of the radiolabeled substrates under the given incubation conditions.

SDS PAGE Analysis of Whole Retinas and Isolated ROS Membranes

Retinas that had been incubated in the presence or absence of TM with either [^{3}H]leucine (Fig. 3) or [^{3}H]mannose (Fig. 4) and ROS membranes derived therefrom were solubilized and analyzed by SDS PAGE and fluorography. In each case, the relative staining intensities of the individual bands document the equivalence of protein loading levels when samples derived from control and TM-incubated tissues are compared. In the ROS samples, the broad, intensely staining component (apparent M_r of 36,000) corresponds to the electrophoretic mobility of opsin (denoted by the asterisk). With the exception of the faint, resolved doublet at M_r 93,000 and another minor component at M_r 230,000, the other ROS membrane components exhibit mobilities typical of opsin aggregates. This

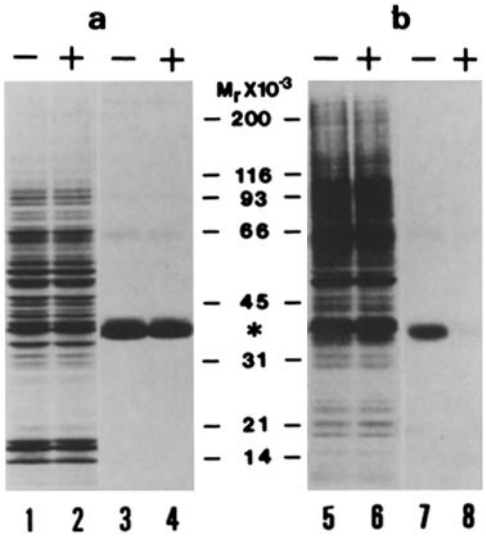

FIGURE 3 SDS PAGE of retinas (lanes *1, 2, 5,* and *6*) and isolated ROS membranes (lanes *3, 4, 7,* and *8*) after incubation with [^{3}H]-leucine in the presence (+) and absence (−) of tunicamycin. (*a*) Coomassie Blue stain, (*b*) fluorograms. Asterisk denotes the electrophoretic migration of opsin (apparent M_r of 36,000). Protein loading levels: retinas, 220 μg; ROS membranes, 45 μg.

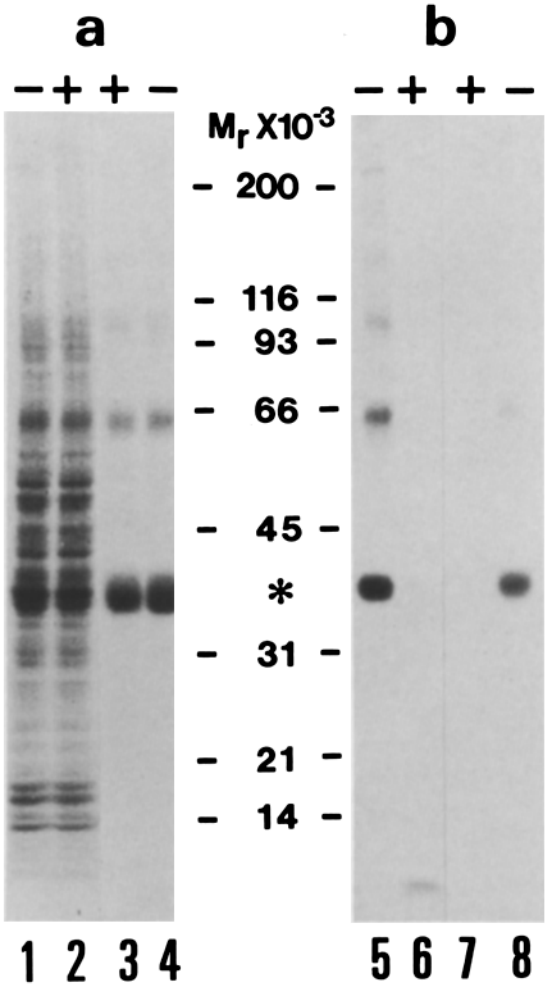

FIGURE 4 SDS PAGE of retinas (lanes *1, 2, 5,* and *6*) and isolated ROS membranes (lanes *3, 4, 7,* and *8*) after incubation with [^{3}H]-mannose in the presence (+) and absence (−) of tunicamycin. (*a*) Coomassie Blue stain; (*b*) Fluorograms. Asterisk denotes electrophoretic migration of opsin (apparent M_r 36,000). Protein loading levels: retinas, 180 μg; ROS membranes, 30 μg.

staining pattern is characteristic of extensively washed, highly purified ROS membranes (41). In the fluorograms obtained from retinas incubated with [^{3}H]leucine there are no observable differences in the relative intensities of corresponding bands of total retinal proteins in the presence (Fig. 3, lane *6*) or absence (Fig. 3, lane *5*) of TM. In particular, the relative intensities of the radiolabeled components in the region of the gel corresponding to the mobility of opsin are virtually identical. These results indicate that TM did not inhibit the synthesis of the various retinal polypeptides, especially opsin, and are in excellent agreement with the data shown in Table I. However, the fluorogram obtained from the ROS membranes derived from retinas incubated with TM (Fig. 3, lane *8*) showed only a very faint band coincident with opsin. In contrast, the control lane (Fig. 3, lane *7*) exhibited a moderately intense band with the electrophoretic mobility of opsin, and some very faint bands with apparent M_r's of 66,000, 93,000, and 230,000. These data suggest that although opsin polypeptides were synthesized in the TM-treated retinas (apparently in amounts similar to controls), most of the newly synthesized molecules were not incorporated into ROS membranes.

In the fluorograms obtained from retinas of companion incubations with [^{3}H]mannose (Fig. 4) there was a striking, almost total absence of radiolabeled components both in total retinal proteins (lane *6*) and ROS proteins (lane *7*) from the TM-incubated tissue as compared with the controls (lanes *5* and *8*, respectively). The only observed radiolabeled component present in the TM-incubated whole retina sample was a very low M_r species, which migrated almost to the dye front of the gel (lane *6*). This component, which did not correspond to any material stainable with Coomassie Blue, may represent a mannolipid species (e.g., dolichylphosphoryl mannose). As previously noted (27), it is a curious but consistent observation that *Xenopus* retinas incubated with [^{3}H]mannose (controls; Fig. 4, lane *5*) incorporate label almost exclusively into opsin and its aggregates, as indicated by the coincidence of the radiolabeled components with the corresponding Coomassie Blue-stained bands in the ROS samples (lanes *3* and *4*). Thus, the *Xenopus* retina presents a rather fortuitous example of a complex tissue composed of multiple cell types in which protein glycosylation is directed with remarkable specificity toward the synthesis of a particular protein species (i.e., opsin). Together, the results presented in Figs. 3 and 4 indicate that, under conditions of normal polypeptide synthesis but marked inhibition of retinal protein glycosylation, opsin is not incorporated into ROS membranes.

Light and Electron Microscopic Autoradiography

We used light microscopic autoradiography to assess the relative distribution of incorporated radioactivity in the various retinal strata and individual cell types after pulse-chase incubations with [^{3}H]mannose or [^{3}H]leucine in the presence or absence of TM. In control retinas incubated with [^{3}H]-mannose (Fig. 5*a*), silver grains were concentrated preferrentially over the outer retina, particularly over photoreceptor inner segments and at the base of the outer segments of rods (indicated by arrows). The inner retinal laminae (not shown) were only sparsely labeled. This relatively selective incorporation of radiolabeled mannose by the photoreceptor cells (particularly rods) has been observed previously (15, 24, 27) and is thought to be indicative of a preferential localization or elevated biogenic activity of the lipid intermediate pathway in the photoreceptor cells relative to other retinal cells (15). The discrete clustering of silver grains forming a band at the base of the ROS is characteristic of the assembly of newly synthesized proteins (in this case mannosylated molecules) during ROS disc membrane morphogenesis (4, 8, 9, 19, 27, 29, 40, 47, 64, 65). In striking contrast, no bands of label were observed at the base of ROS in the retinas incubated in the presence of TM (Fig. 5*b*, arrows), and the relative labeling of RIS (particularly the myoid region) appeared decreased in comparison with the controls. Quantitative light microscopic autoradiography revealed that the silver grain density over the basal ROS compartment was reduced by 85% ($P < 0.01$) relative to controls. However, the distribution of label over other retinal compartments (e.g., cone inner segments, outer nuclear layer, and inner retinal strata) did not appear diminished relative to controls. Electron microscopic autoradiography of the myoid region of an RIS with the adjacent inner segment of a cone taken from a retina incubated with [^{3}H]-mannose in the presence of TM (Fig. 6) revealed a heavy concentration of silver grains over the cone parabaloid appar-

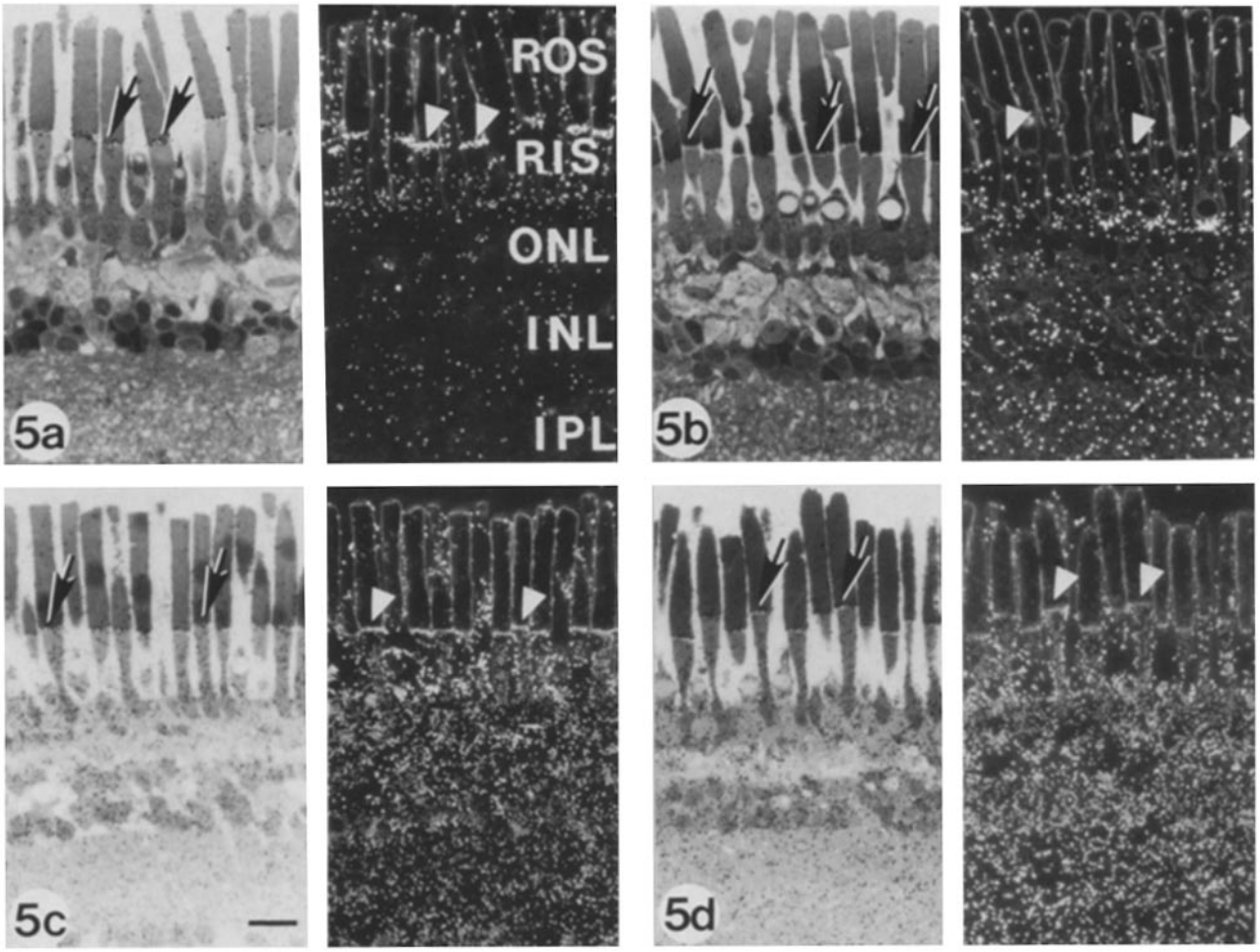

FIGURE 5 Light microscopic autoradiograms (light and dark field) of retinas incubated with [^{3}H]mannose (*a* and *b*) or [^{3}H]leucine (*c* and *d*) in the presence (*b* and *d*) and absence (*a* and *c*) of TM. Arrows denote the basal region of the ROS. Note the bands of silver grains at the base of ROS in control retinas incubated with [^{3}H]mannose and [^{3}H]leucine (*a* and *c*) and TM-treated retinas incubated with [^{3}H]leucine (*d*). The TM-treated retinas incubated with [^{3}H]mannose exhibit no bands of silver grains at the base of ROS (*b*). *ONL*, outer nuclear layer; *INL*, inner nuclear layer; *IPL*, inner plexiform layer. Bar, 10 μm.

ently associated with glycogen deposits distributed throughout that cellular compartment. In contrast, the RIS exhibited a striking paucity of silver grains.

We observed a markedly different labeling pattern when we incubated retinas with [^{3}H]leucine as the radiolabeled substrate, both in the presence (Fig. 5*d*) and absence (Fig. 5*c*) of TM. All retinal strata exhibited extensive incorporation of the radiolabeled substrate, which is indicative of vigorous protein synthesis by all retinal cell types. These results further confirm the biochemical data, which indicate that TM did not appreciably inhibit protein synthesis and that it was not generally cytotoxic under the given incubation conditions. The characteristic bands of silver grains were also observed at the base of the ROS (denoted by arrows), even in retinas incubated with TM. The observation of bands of silver grains over the basal portion of ROS in the TM-incubated retinas seemed to contradict the biochemical evidence, particularly the SDS PAGE data from isolated ROS membranes (Fig. 3), which indicated that newly synthesized proteins (e.g., opsin) were not incorporated into ROS membranes in the presence of TM. We therefore decided to examine by electron microscopic autoradiography the compartments of the rod cell that are involved in the actual assembly of the newly synthesized molecules into disc membranes, i.e., the apical region of the RIS and the basal region of the ROS.

In the rod cells of retinas incubated in the absence of TM with either [^{3}H]leucine (Fig. 7*a*) or [^{3}H]mannose (Fig. 7*b*), a discrete cluster of silver grains was observed over the basal discs of the ROS. Note that the RIS and ROS (joined by the connecting cilium) are separated by an extremely abbreviated extracellular space. However, in retinas incubated in the presence of TM with either [^{3}H]leucine (Fig. 7*c*) or [^{3}H]-mannose (Fig. 7*d*) the extracellular space between the RIS and ROS was substantially distended and was filled with numerous heterogeneously sized vesicles. Although serial sections were not examined, the appearance of these structures was always vesicular, regardless of the orientation of the plane of section through the rod cells. Therefore, we consider these structures to be truly vesicles, as opposed to continuous, tubular elements. Most of the extracellular vesicles appeared to be single walled, and at least two distinct populations were observed: luscent vesicles (*LV*), which appeared either empty or filled with lightly staining material, and dense vesicles (*DV*), which appeared to contain some darker staining material resembling the ROS cytoplasm. Also, the luscent vesicles (mean diameter, 380 nm; range, 237–789 nm) were in general

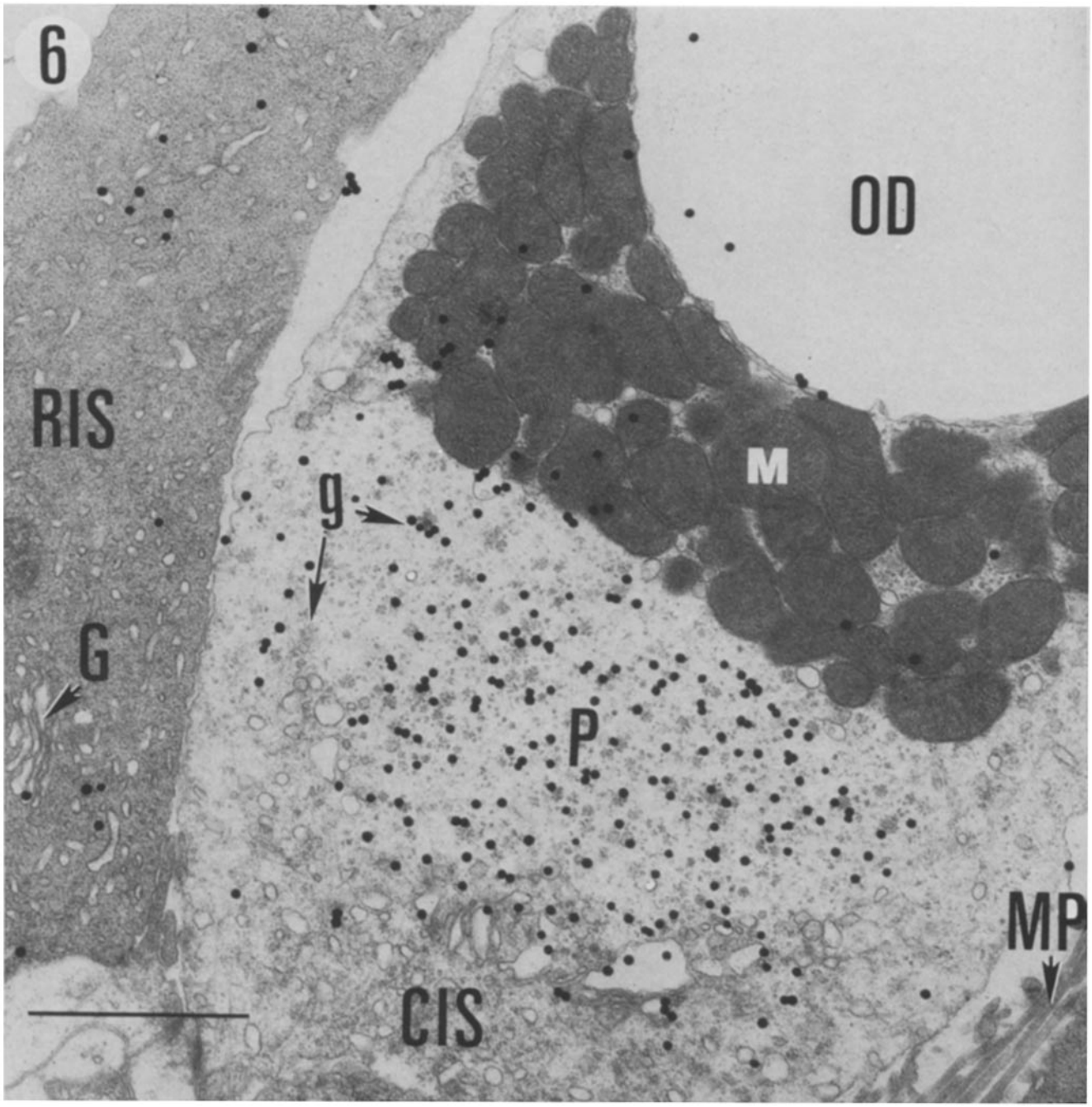

FIGURE 6 Electron microscopic autoradiogram of the inner segments of a cone (*CIS*) and an adjacent rod (*RIS*) from retina incubated with [^{3}H]mannose in the presence of TM. Note the clustering of silver grains over the cone parabaloid (*P*), the site of numerous glycogen deposits (*g*). In contrast, the RIS is only sparsely labeled. *G*, Golgi apparatus; *M*, mitochondrion; *OD*, oil droplet; *MP*, Muller's cell apical processes. Bar, 1 μm.

larger than the dense vesicles (mean diameter, 159 nm; range, 105–237 nm).

The extracellular vesicles in the retinas incubated with [^{3}H]-mannose were not labeled, nor were the basal ROS disc membranes (Fig. 7*d*). In the TM-treated retinas incubated with [^{3}H]leucine (Fig. 7*c*), the silver grains appeared to be most concentrated over the extracellular vesicles rather than over the basal ROS disc membranes. These results indicate that the vesicles that accumulated in the TM-treated retinas, rather than being derived from previously synthesized RIS membrane components or from previously formed ROS disc membranes that had undergone partial degradation and vesiculation, contained newly synthesized proteins that were not glycosylated. Therefore, the apparent contradiction in the results obtained by light microscopic autoradiography and the biochemical data can be reconciled by the fact that the apparent band of label at the base of ROS observed in the light microscopic autoradiograms of TM-treated retinas incubated with [^{3}H]leucine (Fig. 5*d*) actually represents the accumulation of radiolabeled vesicles in the extracellular space between the ROS and RIS and does not represent incorporation of label into the outer segment per se.

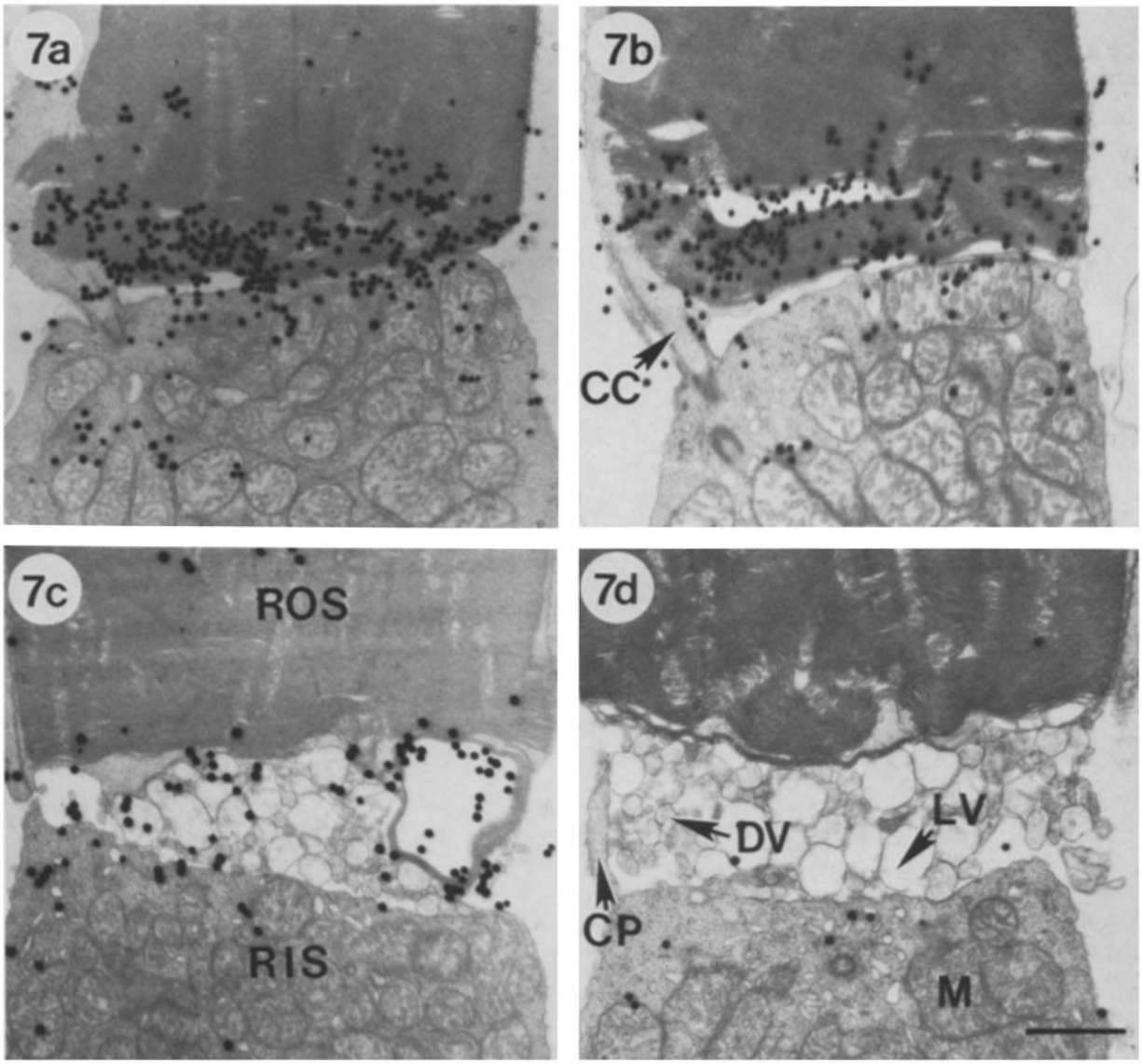

FIGURE 7 Electron microscopic autoradiograms of the basal region of the ROS and the apical region of the RIS in retinas incubated in the presence (*c* and *d*) and absence (*a* and *b*) of TM with either [^{3}H]leucine (*a* and c) or [^{3}H]mannose (*b* and *d*). Note the close apposition of the RIS and ROS, and the clustering of silver grains over the basal ROS discs in the controls (*a* and *b*). The tunicamycin-treated retinas (c and *d*) exhibit an expanded, vesicle-filled space between the RIS and ROS, and the vesicles are loaded with [^{3}H]leucine but not with [^{3}H]mannose. CC, connecting cilium; *CP*, calycal process; *DV*, dense vesicle; *LV*, luscent vesicle; *M*, mitochondrion. Bar, 1 μm.

Time Course for Accumulation of Extracellular Vesicles in TM-incubated Retinas

As shown in Fig. 8, there was a progressive increase in the number of extracellular vesicles trapped between the RIS and ROS of TM-treated retinas as a function of incubation time. After 1 h (Fig. 8*a*), little or no accumulation of vesicles was observed. However, the space between the ROS and RIS was unusually dilated relative to controls. By 2 h (Fig. 8*b*), vesicular material began to appear in the dilated extracellular space and seemed to be more closely associated with the basal surface of the ROS than with the RIS plasma membrane. At this early incubation time electron micrographs that included the connecting cilium within the plane of section (Fig. 9) revealed the presence of vesicle profiles apparently budding off from protrusions of the ciliary plasma membrane (i.e., newly forming open discs) near the base of the ROS. Vesicle accumulation increased over 4 h (Fig. 8*c*) and 6 h (Fig. 8*d*) of incubation, during which time the vesicles appeared to be more uniformly distributed throughout the extracellular space bordered by the inner and outer segments. A survey of numerous rods suggested that there was an expansion of the extracellular space as if to accommodate the increasing amount of vesicular material. The vesicles appeared to be largely confined to the space bordered by the plasma membrane of the RIS and ROS and the network of cytoplasmic projections (the calycal processes), which extends from the RIS longitudinally several microns up the outer perimeter of the ROS. The extracellular space between adjacent photoreceptors contained few, if any, vesicles; however, it is possible

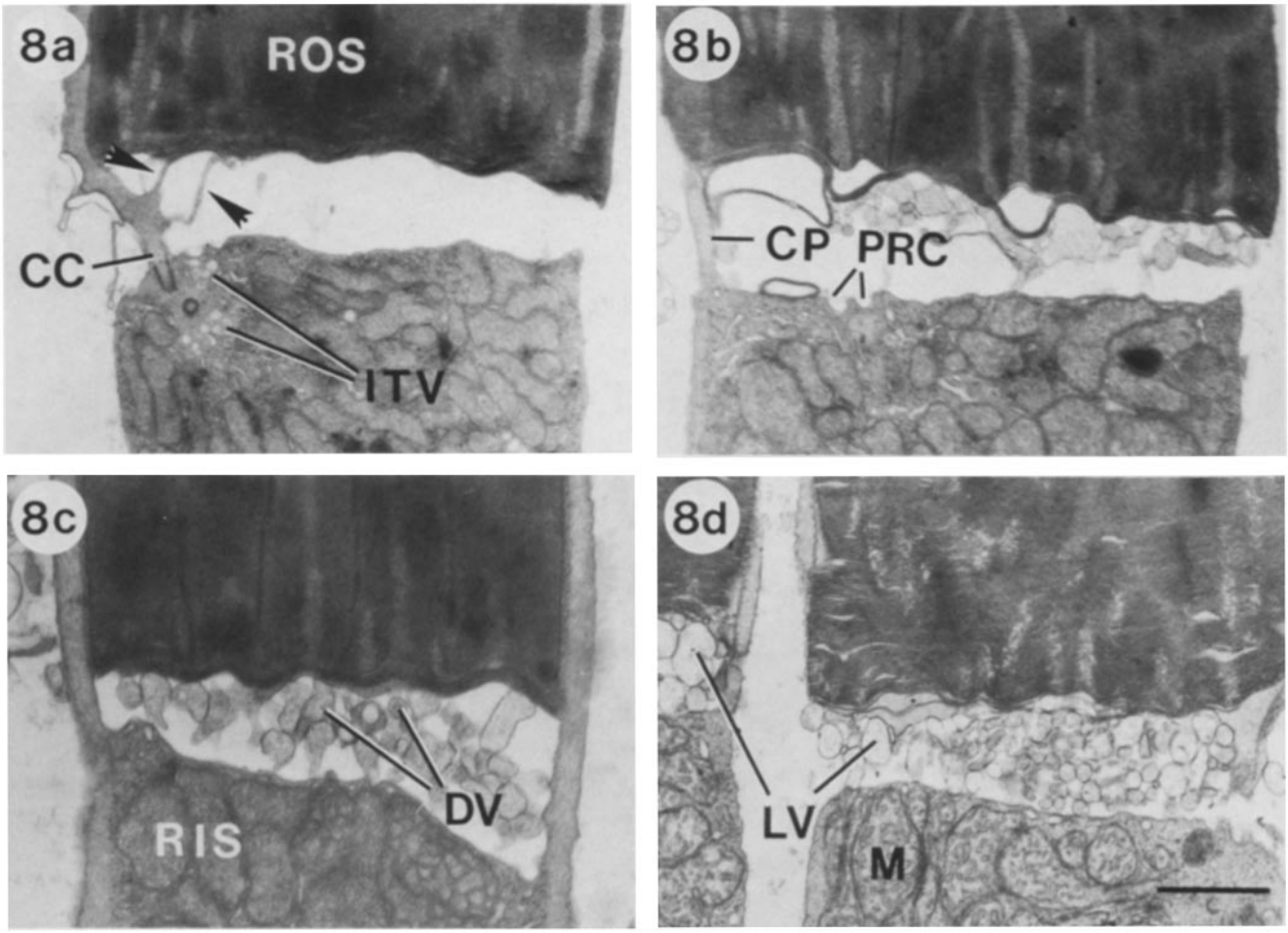

FIGURE 8 Electron micrographs of the basal region of the rod outer segment (*ROS*) and the apical region of the rod inner segment (*RIS*) from retinas incubated in the presence of TM for 1 h (*a*), 2 h (*b*), 4 h (*c*), and 6 h (*d*). Note the dilated space between the RIS and ROS, and the progressive accumulation of dense vesicles (*DV*) and luscent vesicles (*LV*) throughout this space. Arrowheads (a) denote newly forming basal discs evaginating from the connecting cilium (*CC*). *CP*, calycal process; *PRC*, periciliary ridge complex; *M*, mitochondrion. Bar, 1 μm.

that some vesicles escaped from the confines of the photoreceptors and were discarded with the medium during the retrieval of the tissue before fixation.

Effect of TM on Intracellular Transport of Rod Cell Proteins

From the results presented above, it was evident that TM could effectively block the glycosylation of polypeptides destined for ROS membrane assembly, but the precursors were diverted to form membrane vesicles which were then exported from the cell instead of forming normal disc membranes. In an effort to assess whether or not TM affected either the intracellular transport of ROS-destined proteins or the amount of membrane biogenesis devoted to ROS renewal, we pre-incubated retinas in the presence or absence of TM, then performed a 0.5-h pulse-label with [^{3}H]leucine and fixed retinas at various chase times (0.5, 1.5, 2.5, and 3.5 h). Quantitation of silver grains in autoradiograms was performed over the rod cell compartments depicted in the diagram in Fig. 10. It should be noted that, at the light microscopic level, the basal ROS compartment in the TM-treated retinas included the region of accumulation of the extracellular vesicles in addition to the actual basal discs of the ROS.

As shown in Fig. 10, there was no change in grain density over the nucleus, ellipsoid, or distal ROS compartments in either the presence or absence of TM at any stage. This indicated that the distribution of radiolabeled proteins in these rod cell compartments had reached a steady state during the pulse phase that was maintained throughout the incubation. However, there were indications of a gradual loss of radioactivity from the myoid region of the RIS with a compensatory increase in radioactivity in the basal ROS compartment. This type of dynamic labeling pattern reflects the well-documented synthesis of ROS-destined proteins (predominantly opsin) in the myoid, and the subsequent intracellular transport of the proteins through the RIS to their final site of incorporation into the basal ROS compartment (4, 8, 9, 19, 27, 29, 40, 47, 64, 65). In addition, there were no statistically significant differences in the labeling of any of the rod cell compartments analyzed as a function of the presence or absence of TM at a given chase time, including the basal ROS compartment.

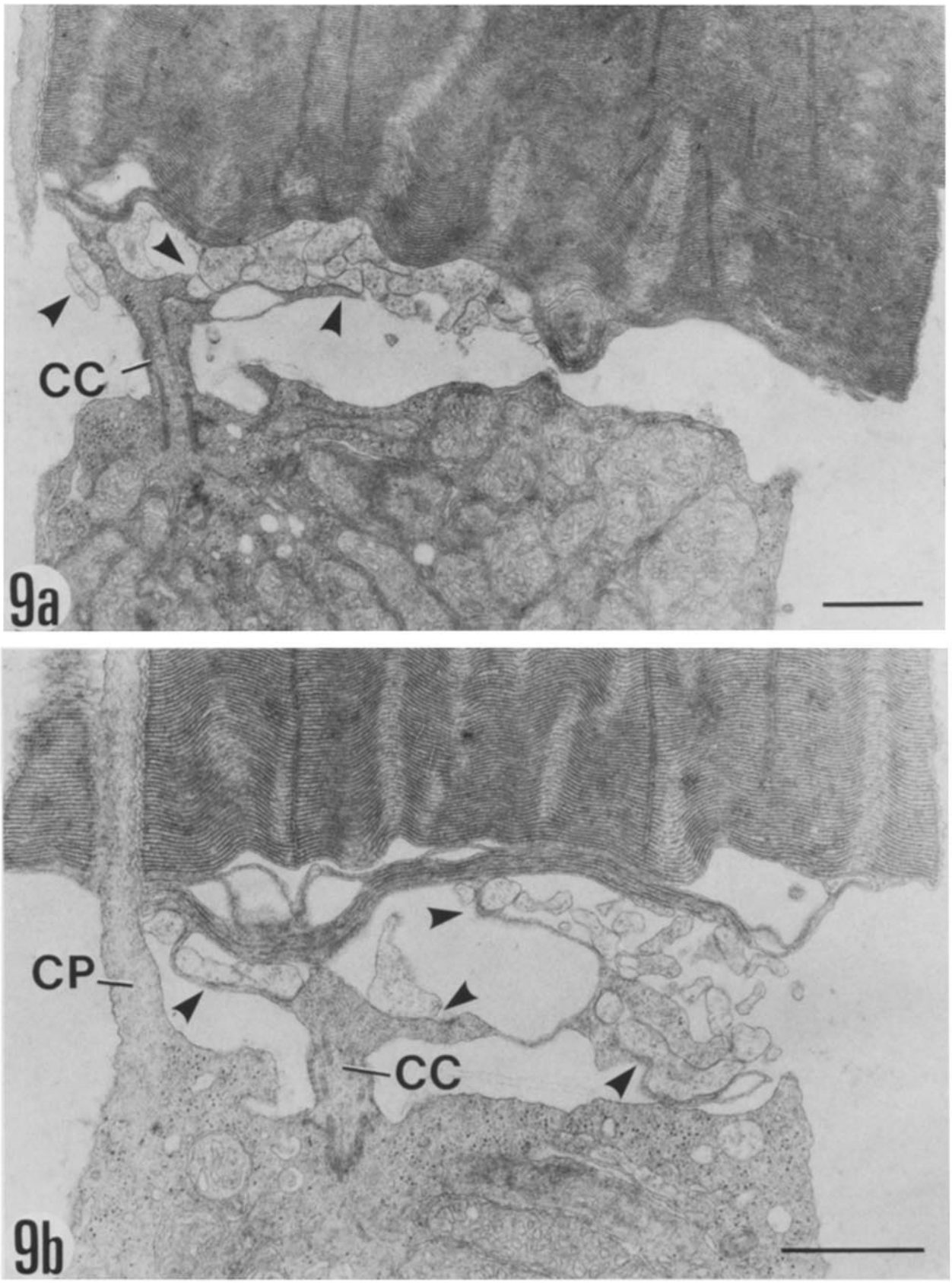

FIGURE 9 Electron micrographs of the inner and outer segment compartments of rod cells taken from retinas that had been incubated for 2 h in the presence of TM. Arrowheads denote the close association of large membrane vesicles with the membrane lamellae (newly forming discs) extending from the connecting cilium (*CC*). Note the presence of a matrix resembling that of the ciliary or ROS cytoplasm within the vesicles. *CP*, calycal process. Bars, 1 μm.

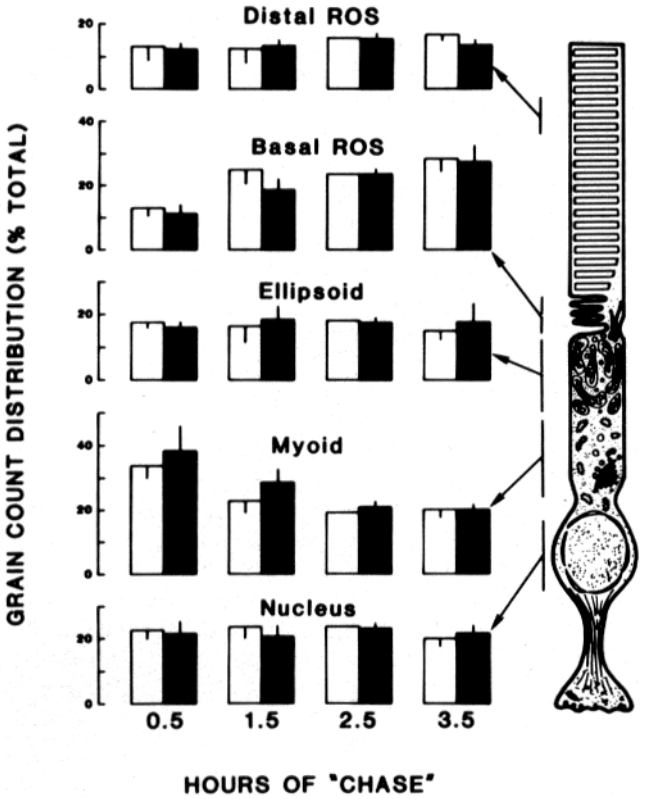

FIGURE 10 Quantitative analysis of silver grain distribution over rod cell compartments as a function of chase time after a 30 min pulse-labeling of retinas with [^{3}H]leucine in the presence (shaded bars) and absence (open bars) of tunicamycin. A schematic diagram of a rod cell is shown at the right side of the figure, illustrating the cellular regions from which grain counts were determined. Values represent the mean ± SD of grain counts taken from three retinas per condition, with three sections per retina and 20 rod cells per section analyzed.

At least three major conclusions can be drawn from these results. First, the rod cell proteins attained the same specific activity in the presence and absence of TM, as the data in Fig. 1 suggested. Second, the flux of these newly synthesized proteins through the inner segment to their sites of incorporation into ROS membranes (in the controls) or extracellular vesicles (in the TM-treated retinas) was nearly identical. That is to say, TM did not substantially affect either the rate or the overall amount of membrane biogenesis devoted to ROS renewal. Rather, the precursors that would normally have been assembled into new disc membranes were instead incorporated into an approximately equivalent amount of material, which was then exported from the cell in the form of membrane vesicles. Third, the data indicate that the presence of the oligosaccharide chains on ROS-destined glycoproteins is not required for routing these products from their site of initial synthesis through the inner segment to the plasma membrane of the cell.

DISCUSSION

The results of this study suggest that glycosylation of ROS-destined proteins with N-linked oligosaccharides is essential in the normal assembly of those products to form ROS disc membranes. Since opsin is, by far, the major glycosylated constituent of the ROS membranes, and TM blocks both the glycosylation of opsin and its incorporation into the ROS, we speculate that the oligosaccharide moieties of opsin play some role in disc membrane morphogenesis. Our results suggest that the rod cell has a mechanism that can distinguish between the glycosylated and nonglycosylated (or aberrantly glycosylated) forms of membrane proteins destined for ROS membrane biogenesis, and that the aberrant precursors can be exteriorized by the cell in the form of membrane vesicles. If the incorporation of such aberrant membrane glycoproteins into the ROS resulted in the formation of physically unstable or functionally incompetent disc membranes, such a mechanism would be very valuable in preserving the structural and functional integrity of the ROS. Although the means by which the cell accomplishes this task remain unclear, some of the possible mechanisms deserve consideration.

The RIS plasma membrane contains a specialized structural feature known as the periciliary ridge complex (1, 50), which presumably serves as the specific site for fusion of ITVs and somehow participates in sorting the newly incorporated membrane constituents for vectorial transport toward their final destinations. In the TM-treated retinas, the extracellular space between the RIS and ROS became unusually dilated and filled with vesicles (Figs. 7 and 8). The fact that these vesicles were labeled with [^{3}H]leucine but not with [^{3}H]mannose indicated that they contained newly synthesized polypeptides that lacked asparagine-linked oligosaccharides. Furthermore, the accumulation of these vesicles exclusively in the space between the ROS and RIS, and the lack of [^{3}H]leucine incorporation into ROS discs per se, indicated that the vesicle material originated in the RIS but that its vectorial transport to the ROS was somehow interrupted. The size (diameter range, 105–789 nm) and form of the extracellular vesicles were markedly different from those of the ITVs commonly observed in the periciliary RIS cytoplasm (mean diameter, 110 nm; range, 50–200 nm). Therefore, it is unlikely that the mechanism of formation of the extracellular vesicles involves the simple fusion and exocytosis of individual ITVs. Although we cannot exclude the possibility that some of the exteriorized membrane material might arise from the inner segment plasma membrane (e.g., by fusion of ITVs with the plasma membrane, coalescence of this additional membrane material to form blebs, and subsequent exocytosis of these blebs from the RIS plasma membrane into the extracellular space), this mechanism does not appear to represent a major source for vesicle formation. The build-up of large extracellular vesicles near the basal region of the ROS and the paucity of these vesicles associated with the RIS plasma membrane argue against such a mechanism. Based on the available data, the most likely mechanism for the TM-induced extracellular vesicle formation is the fusion of multiple ITVs with the RIS plasma membrane, and the subsequent detachment and sloughing of larger membrane blebs from the newly forming basal discs. Profiles of membrane blebs in apparent stages of detachment from newly forming basal discs were observed in electron micrographs that included the connecting cilium within the plane of section (Fig. 9). Furthermore, the matrix material contained within the vesicles more closely resembled the cytoplasm present in the connecting cilium and outer segment than that of the inner segment. This suggests that the newly forming open discs in TM-treated retinas are somehow more labile than those of control retinas, resulting in fragmentation and subsequent vesicle formation before completion and closure of the basal discs. Bleb formation and other

cell surface ultrastructural changes have been observed in cultured cells treated with TM (53). Regardless of the mechanistic details, it is clear that assembly of nonglycosylated opsin to form normal ROS disc membranes does not occur.

In the course of our biochemical investigations, we noted that TM inhibited the incorporation of [^{3}H]mannose into total retinal TCA-precipitable material by only ~66% (Table I), whereas the SDS PAGE analysis of radiolabeled retinal proteins derived from [^{3}H]mannose under the same conditions indicated virtually complete inhibition of incorporation (Fig. 4). Apparently, although protein glycosylation via the lipid intermediate pathway was quantitatively blocked, alternate metabolism of [^{3}H]mannose to TCA-precipitable products was not affected similarly. Microscopic autoradiography of retinas incubated with [^{3}H]mannose in the presence of TM (Figs. 5 and 6) revealed a persistent and prominent incorporation of label in the parabaloids of cones, the region of glycogen storage in those cells. In contrast, RIS were virtually devoid of label. Therefore, this apparent discrepancy might be explained by the TM-insensitive incorporation of [^{3}H]-mannose into radiolabeled glycogen. Since mannose 6-phosphate (derived from mannose via the action of hexokinase) can be converted to glucose 1-phosphate (which then enters the glycogenesis pathway via phosphoglucomutase) (55), [2,6-^{3}H]mannose could be enzymatically converted to [^{3}H]glycogen, with retention of label at carbon-6 of the glucosyl units. In other experiments, we also observed the TM-insensitive incorporation of [2-^{3}H]mannose into cone paraboloids. Since metabolism of [2-^{3}H]mannose to glucosyl units would result in the loss of label at carbon-2 (via a fructose 6-phosphate intermediate) (55), these results suggest that mannose can be incorporated into glycogen without prior conversion to glucose 1-phosphate. Experiments are in progress to pursue this novel observation. In addition, the diffuse, low-level incorporation of [^{3}H]mannose in the inner cell layers of the retina was not appreciably affected by TM. Quantitatively, [^{3}H]-mannose incorporation in cells other than photoreceptors represented only ~15–20% of the total grain counts across the entire retinal expanse in the controls. Therefore, if the inner retina grain counts represented radiolabeled products that were predominantly TCA precipitable but that were not asparagine-linked glycoproteins, this could also contribute to the observed differences in [^{3}H]mannose incorporation when the results obtained by SDS PAGE and TCA precipitation are compared.

In a variety of biological systems, TM has been shown to inhibit protein glycosylation with a concomitant decrease in the apparent M_r of the affected protein, commonly manifested by an increased electrophoretic mobility upon SDS PAGE analysis (56, 63). Plantner et al. (52) noted an apparent ΔM_r of ~2,500 when comparing the SDS PAGE mobilities of radiolabeled bovine opsin with its nonglycosylated form generated by in vitro incubation of retinas with TM. This rather modest shift in the electrophoretic mobility of nonglycosylated bovine opsin relative to the normal protein is a consequence of its two, unusually short asparagine-linked oligosaccharide chains. The structure of the oligosaccharides, primarily $GlcNAcMan_3(GlcNAc)_2$ with lesser $GlcNAcMan_4(GlcNAc)_2$ and $GlcNAcMan_5(GlcNAc)_2$ (16, 20, 33), agrees reasonably well with the carbohydrate composition determined by Plantner and Kean (51). Furthermore, in vitro translation of bovine retina mRNA by use of a wheat germ cell-free system in the absence of dog pancreas microsomes (a source of lipid intermediate glycosylation pathway enzymes) resulted in formation of a nonglycosylated polypeptide (apparent M_r 30,000) which was immunoprecipitable with sheep anti-opsin IgG (18). The major immunoprecipitable product obtained in the presence of microsomes had the electrophoretic and antigenic characteristics of opsin (apparent M_r 36,000) (18), although this product undoubtedly represented opsin molecules that had oligosaccharide moieties somewhat larger than those of normal, fully processed opsin. Incubation of *Rana* retinas with radiolabeled glycoprotein precursors in the presence of TM resulted in the formation of an opsin species (apparent M_r 32,000) with a greater electrophoretic mobility than that of opsin generated in control retinas (apparent M_r 37,000) (12). Unlike in these previous studies, however, our incubations of *Xenopus* retinas with [^{3}H]leucine (Fig. 3) produced no observable shift in the apparent M_r of opsin in TM-treated retinas relative to controls, even though a M_r of 2,000 would have been easily detectable with the gradient SDS PAGE system employed. Since the retinas were incubated at the same time and with the identical culture medium as that used for the companion incubations containing [^{3}H]mannose (where protein glycosylation was markedly inhibited), our results cannot be explained as a failure of TM to block protein glycosylation in those cultures containing [^{3}H]leucine. Although the carbohydrate composition and structures of the oligosaccharide moieties of *Xenopus* opsin have not been determined, these results suggest that they differ from those of bovine opsin in a manner such that the presence or absence of the carbohydrate is of little consequence to the electrophoretic mobility of *Xenopus* opsin.

Since rhodopsin (opsin plus its covalently attached retinaldehyde chromophore) is a cell-specific glycoprotein that is also organelle specific for the ROS, it has been used as a reliable marker for identification and assessment of homogeneity and purity during the isolation of ROS membranes (46). However, the distribution of the apoprotein opsin in various membranous subcellular compartments in the RIS and the potential for artifactual cross-contamination during subcellular fractionation can present problems in the interpretation of pulse-labeling experiments, which use biochemical methods as the sole basis for assigning the subcellular location of newly synthesized opsin molecules. In our ROS preparations from radiolabeled *Xenopus* retinas, there was no apparent cross-contamination with radiolabeled RIS material or with the extracellular vesicle material produced in response to incubation with TM. This suggests that the extracellular vesicles differ somewhat from ROS membranes in their buoyant density, a possibility that might be pursued in further studies to isolate and characterize more extensively the vesicles. Furthermore, although we did not perform these studies with bovine retinas, our results suggest that in the study reported by Plantner et al. (52), the ROS preparations contained radiolabeled RIS-derived material (e.g., extracellular vesicles). The lack of agreement between our results and those of Plantner et al. (52) may be a result of inherent differences in the structural and physical properties of the rods and ROS membranes derived from bovine and *Xenopus* retinas, as well as of variations in the details of the methods employed for isolation of ROS membranes. Our results are in excellent agreement with a recent study that used *Rana* retinas incubated with radiolabeled glycoprotein precursors in the presence or absence of TM (12).

The biological significance of the oligosaccharides of gly-

coproteins remains a matter of considerable speculation (17, 34, 43, 44, 56, 63). One of the putative functions of the carbohydrate moieties is protection of proteins from proteolysis (5, 43, 44). When tissues or cells are cultured in the presence of TM the resulting nonglycosylated forms of glycoproteins are often more susceptible to degradation, as indicated by an increased formation and accumulation of peptide fragments relative to controls. In our experiments, we did not observe the accumulation of low M_r peptides on SDS PAGE of retinas incubated with [^{3}H]leucine in the presence of TM (Fig. 3), nor was the relative intensity or mobility of individual radiolabeled components modified relative to controls. The lack of evidence for increased proteolysis of newly synthesized polypeptides under the given incubation conditions suggests that increased proteolysis was not a significant factor in the lack of incorporation of opsin into ROS membranes in the presence of TM.

Heller (22, 23) proposed that the oligosaccharide chains of opsin might serve to stabilize the normal transmembrane position of the visual pigment in the disc membranes, presumably so as to maintain the 11-*cis* retinaldehyde chromophore in an orientation that is maximally efficient for photon capture. It has also been speculated that opsin's carbohydrate moieties might be involved in the process of disc membrane shedding and/or phagocytosis of the ROS material by the retinal pigment epithelium (21, 37, 40). Our results suggest the novel possibility that the oligosaccharide moieties of opsin exert a major biological function during the process of disc membrane assembly. In general terms, two different kinds of mechanisms might be involved: direct and indirect. Direct interactions would entail specific binding of the carbohydrate chains by one or more other molecular species, e.g. lectins. The participation of endogenous soluble and membrane-associated lectins in both intracellular and intercellular processes has been reviewed recently (2, 3, 44). Lectin–carbohydrate interactions concomitant with the fusion of transport vesicles with the RIS plasma membrane might facilitate sequestration and sorting of ROS-destined precursors before their vectorial transport to the base of the ROS. This hypothesis is a special case of the more general "chemical tag" hypothesis of Olden and co-workers (44), which proposes that protein-bound carbohydrates serve as specific markers that interact with specific intracellular membrane receptors to direct glycoproteins to specific organelles during intracellular transport. The significant variant proposed here is that the carbohydrate chains of opsin do not participate in guiding the visual pigment on its path through the inner segment. Rather, the biologically salient interactions of opsin's oligosaccharides may come into play during the initial phases of ROS membrane assembly once opsin has reached the cell surface. Indirect interactions would not necessarily involve physical contact of the carbohydrate chains per se with other molecules. Instead, the oligosaccharides might affect the conformation of the opsin polypeptide in such a way as to regulate opsin–protein and/or opsin–lipid interactions involved in membrane fusion and subsequent disc morphogenesis. The details of the putative role of opsin's oligosaccharide moieties in ROS membrane assembly remain to be elucidated.

We thank Ms. Janis Rosenthal for technical assistance and Mr. Gary Rutherford for photographic services.

This work was supported by grants from the National Institutes of Health (NIH/NEI), the National Retinitis Pigmentosa Foundation (Baltimore, MD), Research to Prevent Blindness, Inc. (New York, NY), and the Retina Research Foundation (Houston, TX).

Received for publication 30 July 1984, and in revised form 24 October 1984.

REFERENCES

1. Andrews, L. D. 1982. Freeze-fracture studies of vertebrate photoreceptor membranes. *In* The Structure of the Eye. J. G. Hollyfield, editor. Elsevier Biomedical, New York. 11–23.
2. Ashwell, G., and J. Harford. 1982. Carbohydrate-specific receptors of the liver. *Ann. Rev. Biochem.* 51:531–554.
3. Barondes, S. H. 1984. Soluble lectins: a new class of extracellular proteins. *Science (Wash. DC).* 223:1259–1264.
4. Basinger, S. F., and M. O. Hall. 1973. Rhodopsin synthesis *in vitro*. *Biochemistry.* 12:1996–2003.
5. Bernard, B. A., K. M. Yamada, and K. Olden. 1982. Carbohydrates selectively protect a specific domain of fibronectin against proteases. *J. Biol. Chem.* 257:8549–8554.
6. Besharse, J. C., J. G. Hollyfield, and M. E. Rayborn. 1977. Turnover of rod photoreceptor outer segments. I. Membrane addition and loss in relationship to temperature. *J. Cell Biol.* 75:490–506.
7. Besharse, J. C., and K. H. Pfenninger. 1980. Membrane assembly in retinal photoreceptors. I. Freeze-fracture analysis of cytoplasmic vesicles in relationship to disc assembly. *J. Cell Biol.* 87:451–463.
8. Bok, D., S. F. Basinger, and M. O. Hall. 1974. Autoradiographic studies on the incorporation of [6-^{3}H]glucosamine into frog rhodopsin. *Exp. Eye Res.* 18:225–240.
9. Bok, D., M. O. Hall, and P. J. O'Brien. 1977. The biosynthesis of rhodopsin as studied by membrane renewal in rod outer segments. *In* International Cell Biology 1976–1977. B. R. Brinkley and K. R. Porter, editors. The Rockefeller University Press, New York. 608–617.
10. Duksin, D., and W. C. Mahoney. 1982. Relationship of the structure and biological activity of the natural homologues of tunicamycin. *J. Biol. Chem.* 257:3105–3109.
11. Elbein, A. D. 1981. The tunicamycins: useful tools for studies on glycoproteins. *Trends Biochem. Sci.* 6:219–221.
12. Fliesler, S. J., and S. F. Basinger. 1985. Tunicamycin blocks the incorporation of opsin into retinal rod outer segment membranes. *Proc. Natl. Acad. Sci. USA.* In press.
13. Fliesler, S. J., M. E. Rayborn, and J. G. Hollyfield. 1983. Effects of tunicamycin on rod photoreceptor membrane biogenesis. *Invest. Opthalmol. Viscual Sci. (ARVO Suppl.).* 24:279.
14. Fliesler, S. J., M. E. Rayborn, and J. G. Hollyfield. 1983. Tunicamycin disrupts the normal assembly of rod outer segment membranes. *J. Cell Biol.* 94 (*Suppl.* 2): 413a.
15. Fliesler, S. J., G. A. Tabor, and J. G. Hollyfield. 1984. Glycoprotein synthesis in the human retina: localization of the lipid intermediate pathway. *Exp. Eye Res.* 39:153–173.
16. Fukuda, M. N., D. S. Papermaster, and P. A. Hargrave. 1979. Rhodopsin carbohydrate: structure of small oligosaccharides attached at two sites near the NH_2-terminus. *J. Biol. Chem.* 254:8201–8207.
17. Gibson, R., S. Kornfeld, and S. Schlesinger. 1980. A role for oligosaccharides in glycoprotein biosynthesis. *Trends Biochem. Sci.* 5:290–293.
18. Goldman, B. M., and G. Blobel. 1981. In vitro biosynthesis, core glycosylation, and membrane integration of opsin. *J. Cell Biol.* 90:236–242.
19. Hall, M. O., D. Bok, and A. D. E. Bacharach. 1969. Biosynthesis and assembly of the rod outer segment membrane system: function and fate of visual pigment in the frog retina. *J. Mol. Biol.* 45:397–406.
20. Hargrave, P. A. 1982. Rhodopsin chemistry, structure, and topography. *In* Progress in Retinal Research. Vol 1. N. Osborne and G. Chader, editors. Pergamon Press, New York. 1–51.
21. Heath, A. R., and S. F. Basinger. 1983. Simple sugars inhibit rod outer segment disc shedding by the frog retina. *Vision Res.* 23:1371–1377.
22. Heller, J. 1968. Structure of visual pigments. I. Purification, molecular weight and composition of bovine visual pigment$_{500}$. *Biochemistry.* 7:2906–2913.
23. Heller, J., and M. A. Lawrence. 1970. Structure of the glycopeptide from bovine visual pigment$_{500}$. *Biochemistry.* 9:864–869.
24. Hollyfield, J. G., and S. F. Basinger. 1980. Cyclic metabolism of photoreceptors and retinal pigment epithelium in the frog. *Neurochemistry.* 1:103–112.
25. Hollyfield, J. G., J. C. Besharse, and M. E. Rayborn. 1977. Photoreceptor outer segment membranes: accelerated renewal in rods after exposure to light. *Science (Wash. DC).* 196:533–536.
26. Hollyfield, J. G., M. E. Rayborn, P. V. Sarthy, and D. M. K. Lam. 1979. The emergence, localization and maturation of neurotransmitter systems during development of the retina in *Xenopus laevis*. I. Gamma-aminobutyric acid. *J. Comp. Neurol.* 188:587–598.
27. Hollyfield, J. G., M. E. Rayborn, G. E. Verner, M. B. Maude, and R. E. Anderson. 1982. Membrane addition to rod photoreceptor outer segments: light stimulates membrane assembly in the absence of increased membrane biosynthesis. *Invest. Ophthalmol. Visual Sci.* 22:417–427.
28. Kean, E. L. 1980. The lipid intermediate pathway in the retina for activation of carbohydrates involved in the glycosylation of rhodopsin. *Neurochemistry.* 1:59–68.
29. Kinney, M. S., and S. K. Fischer. 1978. The photoreceptors and pigment epithelium of the larval *Xenopus* retina: morphogenesis and outer segment renewal. *Proc. R. Soc. Lond. B Biol. Sci.* 201:149–167.
30. Kornfeld, R., and S. Kornfeld. 1980. Structure of glycoproteins and their oligosaccharide units. *In* The Biochemistry of Glycoproteins and Proteoglycans. W. J. Lennarz, editor. Plenum Press, New York. 1–34.
31. Laemmli, U. K. 1970. Cleavage of structural proteins during the assembly of the head of bacteriophage T4. *Nature (Lond.).* 227:680–685.
32. Lehle, L., and W. Tanner. 1976. The specific site of tunicamycin inhibition in the formation of dolichol-bound *N*-acetylglucosamine derivatives. *FEBS (Fed. Eur. Biol. Soc.) Lett.* 71:167–170.
33. Liang, C. J., K. Yamashita, H. Schichi, C. G. Muellenberg, and A. Kobata. 1979. Structure of the carbohydrate moiety of bovine rhodopsin. *J. Biol. Chem.* 254:6414–6418.
34. Marshall, R. D. 1979. Some observations on why many proteins are glycosylated. *Biochem. Soc. Trans.* 7:800–805.

35. Matheke, M. L., S. J. Fliesler, S. F. Basinger, and E. Holtzman. 1984. The effects of monensin on transport of membrane components in the frog retinal photoreceptor. I. Light microscopic autoradiography and biochemical analysis. *J. Neurosci.* 4:1086–1092.
36. Montreuil, J. 1980. Primary structure of glycoprotein glycans: basis for the molecular biology of glycoproteins. *Adv. Carbohydrate Chem. Biochem.* 37:157–223.
37. O'Brien, P. J. 1976. Rhodopsin as a glycoprotein: a possible role for the oligosaccharide in phagocytosis. *Exp. Eye Res.* 23:127–137.
38. O'Brien, P. J. 1977. Differential effects of puromycin on the incorporation of precursors of rhodopsin in bovine retina. *Biochemistry* 16:953–958.
39. O'Brien, P. J. 1977. Incorporation of mannose into rhodopsin in isolated bovine retina. *Exp. Eye Res.* 24:449–454.
40. O'Brien, P. J. 1978. Rhodopsin: a light-sensitive membrane glycoprotein. *In* Receptors and Recognition. Vol. 6. P. Cuatrecasas and M. F. Greaves, editors. John Wiley & Sons, New York. 109–150.
41. O'Brien, P. J., and C. G. Muellenberg. 1974. The biosynthesis of rhodopsin *in vitro*. *Exp. Eye Res.* 18:241–252.
42. O'Brien, P. J., and C. G. Muellenberg. 1975. Synthesis of rhodopsin and opsin *in vitro*. *Biochemistry.* 14:1695–1700.
43. Olden, K., B. A. Bernard, S. L. White, and J. B. Parent. 1982. Function of carbohydrate moieties of glycoproteins. *J. Cell. Biochem.* 18:313–335.
44. Olden, K., J. B. Parent, and S. L. White. 1982. Carbohydrate moieties of glycoproteins: a re-evaluation of their function. *Biochim. Biophys. Acta.* 650:209–232.
45. Papermaster, D. S., C. A. Converse, and J. Siu. 1975. Membrane biosynthesis in the frog retina: opsin transport in the photoreceptor cell. *Biochemistry.* 14:2438–2442.
46. Papermaster, D. S., and W. J. Dreyer. 1974. Rhodopsin content in the outer segment membranes of bovine and frog retinal rods. *Biochemistry* 13:2438–2444.
47. Papermaster, D. S., and B. G. Schneider. 1982. Biosynthesis and morphogenesis of outer segment membranes in vertebrate photoreceptor cells. *In* Cell Biology of the Eye. D. McDevitt, editor. Academic Press, New York. 475–531.
48. Papermaster, D. S., B. G. Schneider, and J. C. Besharse. 1979. Assembly of rod photoreceptor membranes: immunocytochemical and autoradiographic localization of opsin in smooth vesicles of the inner segment. *J. Cell Biol.* 83 (*Suppl.* 2):275a.
49. Papermaster, D. S., B. G. Schneider, M. A. Zorn, and J. P. Kraehenbuhl. 1978. Immunocytochemical localization of opsin in the outer segments and Golgi zones of frog photoreceptor cells. *J. Cell Biol.* 77:196–210.
50. Peters, K.-R., G. E. Palade, B. G. Schneider, and D. S. Papermaster. 1983. Fine structure of a periciliary ridge complex of frog retinal rod cells revealed by ultrahigh resolution scanning electron microscopy. *J. Cell Biol.* 96:265–276.
51. Plantner, J. J., and E. L. Kean. 1976. Carbohydrate composition of bovine rhodopsin. *J. Biol. Chem.* 251:1584–1552.
52. Plantner, J. J., L. Poncz, and E. L. Kean. 1980. Effect of tunicamycin on the glycosylation of rhodopsin. *Arch. Biochem. Biophys.* 201:527–532.
53. Pratt, R. M., K. M. Yamada, K. Olden, S. Ohanian, and V. C. Hascall. 1979. Tunicamycin-induced alterations in the synthesis of sulfated proteoglycans and cell surface morphology in the chick embryo fibroblast. *Exp. Cell. Res.* 118:245–252.
54. Schachter, H. 1978. Glycoprotein synthesis. *In* The Glycoconjugates. Vol. 2. M. I. Horowitz and W. Pigman, editors. Academic Press, New York. 87–181.
55. Schwartz, N. B. 1982. Carbohydrate metabolism. II. Special pathways. *In* Textbook of Biochemistry with Clinical Correlations. T. M. Devlin, editor. John Wiley & Sons, New York. 414–415.
56. Schwartz, R. T. and R. Datema. 1982. The lipid intermediate pathway of protein glycosylation and its inhibitors: the biological significance of protein-bound carbohydrates. *Adv. Carbohydrate Chem. Biochem.* 40:287–379.
57. Steinberg, R. H., S. K. Fischer, and D. H. Anderson. 1980. Disc morphogenesis in vertebrate photoreceptors. *J. Comp. Neurol.* 190:501–518.
58. Struck, D. K., and W. J. Lennarz. 1977. Evidence for the participation of saccharide-lipids in the synthesis of the oligosaccharide chain of ovalbumin. *J. Biol. Chem.* 252:1007–1013.
59. Struck, D. K., and W. J. Lennarz. 1980. The function of saccharide-lipids in synthesis of glycoproteins. *In* The Biochemistry of Glycoproteins and Proteoglycans. W. J. Lennarz, editor. Plenum Press, New York. 35–83.
60. Takatsuki, A., K. Kohno, and G. Tamura. 1975. Inhibition of biosynthesis of polyisoprenol sugars in chick embryo microsomes by tunicamycin. *Agric. Biol. Chem.* 39:2089–2091.
61. Tkacz, J. S., and J. O. Lampen. 1975. Tunicamycin inhibition of polyisoprenyl-*N*-acetylglucosaminyl pyrophosphate formation in calf liver microsomes. *Biochem. Biophys. Res. Commun.* 65:248–257.
62. Udenfriend, B., S. Stein, B. Bohlen, W. Dairman, W. Leingruber, and M. Weigele. 1972. Fluorescamine: a reagent for assay of amino acids, peptides, proteins and primary amines in the picomole range. *Science (Wash. DC).* 178:871–872.
63. Yamada, K. M., and K. Olden. 1982. Action of tunicamycin on vertebrate cells. *In* Tunicamycin. G. Tamura, editor. Japan Scientific Societies Press, Tokyo. 119–144.
64. Young, R. W. 1967. The renewal of photoreceptor cell outer segments. *J. Cell Biol.* 33:61–72.
65. Young, R. W. 1976. Visual cells and the concept of renewal. *Invest. Ophthalmol.* 15:700–725.